Research Paper

Observer-Based Prescribed Time Bipartite Formation-Containment Tracking Control for Layered Multi-agent Systems under Signed Digraphs

Kaiyin Huang, Tao Li, Jialong Tian, Zijie Jiang, Haiyang Hu, Yuqi Gao

School of Electrical Engineering and Automation, Hubei Normal University, Huangshi 435002, China
Corresponding Author: Tao Li

ABSTRACT:*This paper investigatesthe prescribedtime bipartite formation-containment tracking control for the layered multi-agent systems (MASs) under the signed digraphsbased on the observer. In this system, the leader layer track the trajectory of the tracking leader and engages in a purely cooperative relationship, while the follower layer engages in both cooperation and competition. Moreover, there exists a restraining relationship between the leader layer and corresponding follower layer. By introducing a time-varying function, a distributed prescribedtime observer is designed for the leader layer to accuratelyestimation of the tracking leader's state within the prescribed time. A novel prescribedtime distributed control protocol is designed to drive leader layer to approach the tracking leader and form a formation within a prescribed time, while the follower layer simultaneously converges into the convex hulls formed by the states and the sign-inverted states of the leader layer. By using graph theory and Lyapunov stability theory, the validity of the designed control protocol is proved in detail, and the corresponding sufficient conditions for the prescribed time stability of the MASs are derived. Finally, a simulation example confirms the effectiveness of the analytical results.*

KEYWORDS: *Layered multi-agent systems;Observer;Prescribedtime control; Bipartite formation-containment;Signed digraphs*

I. INTRODUCTION

In the last 20 years, a large amount of literature has been devoted to investigating the emergence of cooperative behaviors such as consensus [1], [2] and synchronization over multi-agent systems(MASs) which have good expansibility to formation tracking [3-5], containment control [6], [7] and formation-containment control [8-10].

As one of the most critical cooperative behaviors in multi-agent network, formation-containment of MASs has been studied under various scenarios in the past decades including formation-containment of MASs with second-order dynamics [11], [12], formation-containment of MASs with general linear dynamics [13], formation-containment of MASs with sliding mode control [14], formation-containment under adaptive event-triggered strategies [15], and Finite-horizon robust formation-containment [16], to mention just a few. The aforementioned works, however, were derived under cooperative networks, meaning agents have only cooperative relationships with their neighbors. In many realworld scenarios such as social networks and biological systems, different individuals have varying perspectives on the same issue, resulting in competitive relationships between them. And then generate signed networks [17], [18] which can be characterized by graphs that accommodate not just positive, but also negative adjacency weights. Bipartite consensus was first proposed in [19], the term "bipartite" indicates that all states tend to be equal in magnitude but opposite in sign. Studying MASs under signed networks is more practically meaningful.

It is important to note that all the aforementioned works on formation containment control concentrate on the analysis and application of synchronization in single-layer complex dynamical networks, which may oversimplify certain real-world systems. Unlike MASs with a single layer, the practical applications of layered MASs in real-world domains have garnered significant attention from researchers. This heightened interest is due to the potential advantages of layered MASs in modeling real-world networks, such as power grids and

social media networks. In aforementioned formation containment control studies, the follower be required to track the convex combination of all leaders' states, rather than the states of a particular leader. These mean that the follower's behavior and control inputs are influenced by the states of all leaders. However, this consideration of localized interactions between leaders and followers does not align with certain real-world scenarios. For example, in the multi-robot systems, the follower robot may need to closely follow a specific leader robot while disregarding the movements of other leader robots. Building upon these observations and the concept of consensus tracking, Wen et al.[20] introduced the notion of node-to-node consensus. Scholars have carried out theoretical research on MASs in two-layered networks [21], [22]. In this framework, MASs are composed of two layers: a leader layer and a follower layer. Each layer consists of an equal number of agents, and during the evolution of the systems, certain agents in the follower layer are "pinned". The layered MASs can achieve the global objective of the networks by designing a local control strategy within each layer. This approach significantly reduces the complexity of the network model design. Therefore, it is meaningful to discuss the formation containment control problem of MASs in layered network.

In real-world applications, convergence time is an essential criterion for evaluating the effectiveness of distributed control algorithms. Initially, the convergence time of the distributed control and observer algorithms is infinite, which implies that the convergence speed of the system can be slow and even unpredictable. This consequently motivates the development of finite-time distributed control and observer algorithms to achieve various collective behaviors, including formation tracking [23], formation containment tracking [24]. In the reference [25], several innovative finite-time and fixed-time average tracking algorithms have been introduced, effectively addressing the fast distributed average tracking problem of MASs. In the reference [26], the fixed-time formation tracking control problem for MASs with model uncertainties and no leader's velocity measurements has been addressed by using a novel fixed-time cascaded leader state observer. Note that the convergence time of all the above-mentioned results is determined by the initial condition and the control parameters. Ensuring a short completion time is vital for certain time-sensitive applications, such as multi-missile cooperative attacks. As a result, the prescribedtime algorithms for controlling and observing, which is able to specify the convergence time by the designer via the parameters in the controller and observer, was developed recently and has received considerable attention [27].

The above observations inspire us to tackle the challenge of prescribedtime formation bipartite containment of two-layered second-order MASs. This paper presents a novel prescribedtime observer-based control algorithms for formation bipartite containment of two-layered MASs in which the finite convergence time can be explicitly prespecified. Ultimately, the states of the leader layer form a predefined formation while tracking the state of the leader within the specified time, while the followers achieve convergence within the convex hulls formed by the states as well as the sign-inverted states of the leaders at the same time.

The rest parts of this paper are organized as follows: Section 2 offers crucial background information on graph theory and matrix theory, alongside the formulation of the model. The main analytical findings are detailed in Section 3. A numerical example is provided in Section 4 to illustrate the effectiveness of the analytical results, followed by conclusions in Section 5.

II.PRELIMINARIES AND STATEMENT OF PROBLEM

2.1 GRAPH THEORY

Consider MASs with 2n+1 agents, which consisting of one tracking leader,a leader layer and a follower layer,each layer contains n agents.

Let $G_L = (V^L, \varepsilon^L, B)$ represent the communication topology of the leaders, which is a directed non-negative graph with n nodes. Here, $V^L = \{v_1^L, v_2^L, L, v_n^L\}$ represents the node set, where the indices of nodes belong to $\varpi = \{1, 2, L, n\}$; $\varepsilon^L = \{(j,i) : b_{ij} > 0\}$ represents the edge set, where a_{ij} denotes the weight of edge (j,i); $A = [a_{ij}] \in R^{n \times n}$ is the adjacency matrix, where $a_{ij} \geq 0$. The $G_F = (V^F, \varepsilon^F, A)$ represent the communication topology of the followers, which is a symbolic graph with n nodes, $V^F = \{v_1^F, v_2^F, L, v_n^F\}$ represents the node set, $\varepsilon^F = \{(j,i) : a_{ij} \neq 0\}$ represents the edge set, where b_{ij} denotes the weight of edge (j,i). $A = [a_{ij}] \in R^{n \times n}$ is the adjacency matrix, where $b_{ij} > 0$ indicates a positive connection (cooperation) between agent nodes i and j, $b_{ij} < 0$ indicates a negative connection (competition) between agent nodes i and j, and $b_{ij} = 0$ indicates no connection between agent nodes i and j.Moreover, the matrix $g = diag\{g_1, L, g_n\}$ is utilized to depict the interaction between the leader and the ith follower. $g_i > 0$ indicates direct information flow from the leader to the ith follower and $g_i = 0$ otherwise.Let the Laplacian matrices of graphs G_L and G_F be denoted as $L_L = [l_{ij}^L] \in R^{n \times n}$ and $L_F = [l_{ij}^F] \in R^{n \times n}$, they are written as:

$$l_{ij}^L = \begin{cases} \sum_{k=1}^n a_{ik} & , i=j \\ -a_{ik} & , i \neq j \end{cases} \qquad , l_{ij}^F = \begin{cases} \sum_{k=1}^n |b_{ik}| & , i=j \\ -b_{ij} & , i \neq j. \end{cases}$$

Let q_j represent the weight assigned to the pinning edges connecting the leader j and the follower j, $j = 1,2,\text{L}, n$. By relabeling the leader layer as a single agent 0, we can reconstruct a graph G which its Laplacian matrix can be expressed as follows:

$$L = \begin{pmatrix} 0 & 0_n^T \\ -Q & \Lambda \end{pmatrix},$$

where $Q = [p_1, \text{L}, p_n]^T$, $\Lambda = L_F + q$, $q = diag\{q_1, \text{L}, q_n\}$, $\Lambda_l = g + L_L$.

2.2 SOME LEMMAS AND DEFINITIONS

Assumption 1 In the directed graph G, there exists a spanning tree where the root serves as the leader. This implies that there is at least one directed path from the leader to each follower.

Before moving on, our control laws will be subjected to a time-varying scaling function, taking the following form:

$$\chi(t) = (\frac{T_K}{t_0 + T_K - t})^\rho, t \in [t_0, t_0 + T_K],$$

in which $\rho > 1$, t_0 and $T_K > 0$ are the initial time and user-specified constant.

Assumption 2 At each time instant $t \geq t_0$, $\varepsilon^F \subset \varepsilon^L$.

Lemma 1 Consider a system characterized by

$$\dot{q}(t) = f(t, q(t)), \; q_0 = q(0). \tag{1}$$

Where $q(t) \in R^m$ is the state and $f : R_+ \times R^m \to R^m$ is a vector field bounded in time.

There exists a valid Lyapunov function $V(t, q(t))$ with $V(t, 0) = 0$ for (1), we use V to denote $V(t, q(t))$, if it such that

$$\dot{V} \leq -cV - d\varphi(t)V, \; t \in [t_0, t_0 + T_K]. \tag{2}$$

with $c \geq 0$, $d \geq 0$ being two constants and $\varphi(t)$ being defined as

$$\varphi(t) = \begin{cases} \dfrac{\dot{\chi}(t)}{\chi(t)}, t_0 \leq t < t_0 + T_K, \\ \dfrac{\rho}{kT}, t \geq t_0 + T_K, \end{cases}$$

then for $t \in [t_0, t_0 + T_K]$, it yields

$$\begin{cases} V \leq \chi(t)^{-k} \exp(-c(t-t_0))V(q_0), t \in [t_0, t_0 + T_K) \\ V \equiv 0, t \in [t_0 + T_K, \infty). \end{cases}$$

Lemma 2 There exists a positive define matrix $M = diag(y_i / x_i)$ such that $N = M\Lambda + \Lambda^T M$ is positive define, where $y = [y_1, y_2, \text{L}, y_N] = \Lambda^{-T} 1_N$, $x = [x_1, x_2, \text{L}, x_N] = \Lambda^{-1} 1_N$, and $\Lambda = L_f + q$, $q = diag\{q_1, \text{L}, q_n\}$.

2.3 PROBLEM STATEMENT

Consider MASs with 2n+1 agents, which consisting of one tracking leader, n formation leaders, and n followers. Consider the tracking leader agent with dynamics as follow:

$$\begin{aligned} \dot{x}_0(t) &= v_0(t) \\ \dot{v}_0(t) &= u_0(t) \end{aligned} \tag{3}$$

where x_0, $v_0 \in R^m$ are the position and velocity of the leader, respectively, u_0 is the control input or the acceleration of the leader.

The dynamics of the formation leaders are indicated as:

$$\begin{cases} \dot{x}_{Li}(t) = v_{Li}(t) \\ \dot{v}_{Li}(t) = u_{Li}(t) \end{cases} \tag{4}$$

where the position $x_{li}(t) \in R^m$, the velocity $v_{li} \in R^m$, and $u_{li}(t) \in R^m$ is the control input.

The dynamics of the followers are indicated as:

$$\begin{cases} \dot{x}_{Fi}(t) = v_{Fi}(t) \\ \dot{v}_{Fi}(t) = u_{Fi}(t) \end{cases} \tag{5}$$

where the position $x_{fi}(t) \in R^m$, the velocity $v_{fi} \in R^m$, and $u_{fi}(t) \in R^m$ is the control input.

Definition 1 The prescribedtime formation bipartite containment tracking problem of the second-order MASs is solved if the errors converge to zero within the prescribedtime T, namely,

$$\begin{cases} \lim_{t \to T} \|x_{Li}(t) - x_0 - h_i\| = 0 \\ \|x_{Li}(t) - x_0 - h_i\| = 0, \forall t > T \\ \lim_{t \to T} \|v_{Li}(t) - v_0\| = 0 \\ \|v_{Li}(t) - v_0\| = 0, \forall t > T \\ \lim_{t \to T} \left\| x_{Fk}(t) - \sum_{j=1}^{n} (\alpha_{kj} x_{Lj}(t) - \beta_{kj} x_{Lj}(t)) \right\| = 0, k = 1, 2, \mathrm{L}, n \\ \left\| x_{Fk}(t) - \sum_{j=1}^{n} (\alpha_{kj} x_{Lj}(t) - \beta_{kj} x_{Lj}(t)) \right\| = 0, \forall t > T \end{cases} \tag{6}$$

where $T > 0$ is an arbitrary time-independent constant, and h_i is the offset from the *ith* agent to the center of the formation shape. Nonnegative constants $\alpha_{kj} \geq 0, \beta_{kj} \geq 0 (j = 1, 2, \mathrm{L}, n)$ satisfying $\sum_{j=1}^{n} (\alpha_{kj} + \beta_{kj}) = 1$.

III.CONTROL PROTOCOL DESIGN AND STABILITY ANALYSIS

In practical applications, it is unrealistic to assume that all the followers have access to the states of the leader. The leader's states x_0 and v_0 are only accessible to the followers that are adjacent to the leader. Therefore, we construct a distributed observer for formation leader *i* to estimate the tracking leader's states. In **Error! Reference source not found.**, a prescribedtime observer was designed as

$$\begin{cases} \dot{\varsigma}_{vi} = u_0 - \beta(c_1 + d_1\varphi_1(t))\delta_{1i} \\ \dot{\varsigma}_{xi} = -\beta(c_1 + d_1\varphi_2(t))\delta_{2i} \end{cases} \tag{7}$$

where $\delta_{1i} = \sum_{j=1}^{N} a_{ij}(\varsigma_{vi} - \varsigma_{vj}) + b_i(\varsigma_{vi} - v_0)$, $\delta_{2i} = \sum_{j=1}^{N} a_{ij}(\varsigma_{xi} - \varsigma_{xj}) + b_i(\varsigma_{xi} - x_0)$, ς_{xi}, ς_{vi} are the observed states of x_0, v_0, respectively. β, F_m are the observer gains, c, d are the control parameters. $\varphi_k(t)$ ($\forall k = 1, 2, 3$) is defined as

$$\varphi_k(t) = \begin{cases} \dfrac{\dot{\chi}_k(t)}{\chi_k(t)}, t_0 \leq t < t_0 + kT_K, \\ \dfrac{\rho}{kT}, t \geq t_0 + kT_K, \end{cases}$$

where $\chi_k(t) = \left(\dfrac{kT_K}{t_0 + kT_K - t} \right)^{\rho}, t \in [t_0, t_0 + kT_K]$.

Having completed the aforementioned preparation, we are now able to introduce the prescribedtime control protocol control protocol. The control protocols for leaders and followers are designed separately:

$$u_{li}(t) = -k_{L1}\varphi_3^2(t)(\sum_{j=1}^{N} a_{ij}((x_{Li} - h_i) - (x_{Lj} - h_j)) + g_i(x_{Li} - x_0 - h_i))$$
$$-k_{L2}\varphi_3(t)(\sum_{j=1}^{N} a_{ij}(v_{Li} - v_{Lj}) + g_i(v_{Li} - v_0)) + u_0$$

(8)

$$u_{fi}(t) = -k_{F1}\varphi_3^2(t)(\sum_{j=1}^{N} b_{ij}(sign(b_{ij})x_{Fi} - x_{Fj}) + q_i(sign(q_i)x_{Fi} - x_{Li}))$$
$$-k_{F2}\varphi_3(t)(\sum_{j=1}^{N} b_{ij}(sign(b_{ij})v_{Fi} - v_{Fj}) + q_i(sign(q_i)v_{Fi} - v_{Li}))$$
$$+(\Lambda^{-1}p \otimes I_m)_i u_{li}(t)$$

(9)

Theorem 1. Suppose that Assumptions 1 hold. By using the prescribedtime observer-based control algorithm, if

$$\beta \geq \varepsilon_2,$$
$$\frac{2}{\rho} \leq d \leq \frac{K_{L1}}{K_{L2}},$$
$$K_{L1}\varepsilon_2 - K_{L2}^2 < 0,$$
$$K_{F1}\varepsilon_2 - K_{F2}^2 < 0,$$
$$\varepsilon_1(3cT + d\rho + 1) + K_{L2}(2 + 3cT + d\rho) - \rho K_{L1} < 0,$$
$$\varepsilon_2[K_{L1}(2\rho + 1) + (3cT + d\rho)(K_{L1} + K_{L2})] - \rho K_{L2}^2 < 0,$$
$$\varepsilon_1(3c_2T + d_2\rho + 1) + K_{F2}(2 + 3c_2T + d_2\rho) - \rho K_{F1} < 0,$$
$$\varepsilon_2[K_{F1}(2\rho + 1) + (3c_2T + d_2\rho)(K_{F1} + K_{F2})] - \rho K_{F2}^2 < 0,$$

(10)

then the predefined-time control protocol tracking errors converge to zero within $T = t_0 + 3T_K$, where $c_2, c \geq 0$,
$d_2, d \geq 0$, $\varepsilon_1 = \frac{\lambda_{max}(M)}{\lambda_{max}(N)}$, $\varepsilon_2 = \frac{\lambda_{max}(M)}{\lambda_{min}(N)}$.

Proof: After $t \geq 2T_K$, the information of the target's states x_0 and v_0 can be obtained by formation leaders. Firstly, it is proven to achieve formation tracking control within T.

Let $\overset{\backslash}{x}_{Li} = x_{Li} - x_0 - h_i$, $\overset{\backslash}{v}_{Li} = v_{Li} - x_0$, $\overset{\backslash}{x}_L = col(\overset{\backslash}{x}_{L1}, \overset{\backslash}{x}_{L2}, \text{L}, \overset{\backslash}{x}_{Ln})$, $\overset{\backslash}{v}_{Li} = col(\overset{\backslash}{v}_{L1}, \overset{\backslash}{v}_{L2}, \text{L}, \overset{\backslash}{v}_{Ln})$. Define two auxiliary states as $\overset{\backslash}{x}_{Li} = \varphi_3(t)\overset{\backslash}{x}_{Li}$, $\overset{\backslash}{v}_{Li} = \overset{\backslash}{v}_{Li}$. By deriving $\overset{\backslash}{x}_{Li}$, it results in

$\overset{\&}{x}_{Li} = \overset{\backslash}{\phi}_3(t)\overset{\backslash}{x}_{Li} + \varphi_3(t)\overset{\backslash}{v}_{Li}$, where

$$\overset{\backslash}{\phi}_3(t) = \frac{\overset{\backslash}{\phi}_3(t)}{\varphi_3(t)} = \begin{cases} \frac{\varphi_3(t)}{\rho}, t_0 \leq t < t_0 + 3T_K \\ 0, t \geq t_0 + 3T_K. \end{cases}$$

(11)

Therefore, it can be derived that

$$\begin{cases} \overset{\&}{x}_L = \overset{\backslash}{\phi}_3(t)\overset{\backslash}{x}_L + \varphi_3(t)\overset{\backslash}{v}_L \\ \overset{\&}{v}_L = -\varphi_3(t)(\Lambda_l \otimes I_m)(k_{L1}\overset{\backslash}{x}_L + k_{L1}\overset{\backslash}{v}_L) \end{cases}$$

(12)

where $\overset{\backslash}{x}_L = col(\overset{\backslash}{x}_{L1}, \overset{\backslash}{x}_{L2}, \text{L}, \overset{\backslash}{x}_{Ln})$, $\overset{\backslash}{v}_L = col(\overset{\backslash}{v}_{L1}, \overset{\backslash}{v}_{L2}, \text{L}, \overset{\backslash}{v}_{Ln})$, $\Lambda_l = g + L_L$. Define $X = [\overset{\backslash}{x}_L^T, \overset{\backslash}{v}_L^T]^T$, it follows that $\overset{\&}{X} = \Theta X$, where

$$\Theta = \begin{bmatrix} \overset{\backslash}{\phi}_3(t)I_n & \varphi_3(t)I_n \\ -k_{L1}\varphi_3(t)\Lambda_l & -k_{L2}\varphi_3(t)\Lambda_l \end{bmatrix} \otimes I_m$$

The Lyapunov function candidate is formulated as $V_1 = \frac{1}{2} X_L^T (\Omega \otimes I_m) X_L$, where

$$\Omega = \begin{bmatrix} k_{L1} N & \dfrac{k_{L1}}{k_{L2}} M \\[2ex] \dfrac{k_{L1}}{k_{L2}} M & M \end{bmatrix},$$

M, N are defined in Lemma 2. According to Lemma 2, M is positive define, then based on the fourth inequality of (12), it follows that $V_1 \geq 0$. By taking the derivative of V_1, we obtain that

$$
\begin{aligned}
\dot{V}_1 = & \frac{k_{L1}}{\rho} \varphi_3(t) \dot{x}_L^T (N \otimes I_m) \dot{x}_L - \frac{k_{L1}}{k_{L2}} \varphi_3(t) \dot{x}_L^T (\Lambda_l M \otimes I_m) \dot{x}_L \\
& + \frac{k_{L1}}{k_{L2}} \varphi_3(t) \dot{v}_L^T (M \otimes I_m) \dot{v}_L - k_{L2} \varphi_3(t) \dot{v}_L^T (M \otimes I_m) \dot{v}_L \\
& + \dot{x}_L^T (k_{L1} \varphi_3(t)(N \otimes I_m) + \frac{k_{L1}}{k_{L2}\rho} \varphi_3(t)(M \otimes I_m)) \dot{v}_L - k_{L1} \varphi_3(t) \dot{x}_L^T (N \otimes I_m) \dot{v}_L
\end{aligned}
\tag{13}
$$

Utilizing Lemma 2, the following equality holds.

$$
\begin{aligned}
\frac{k_{L1}^2}{k_{L2}} \varphi_3(t) \dot{x}_L^T (\Lambda_l M \otimes I_m) \dot{x}_L &= \frac{k_{L1}^2}{2k_{L2}} \varphi_3(t) \dot{x}_L^T (N \otimes I_m) \dot{x}_L \\
k_{L2} \varphi_3(t) \dot{v}_L^T (\Lambda_l M \otimes I_m) \dot{v}_L &= \frac{k_{L2}}{2} \varphi_3(t) \dot{v}_L^T (N \otimes I_m) \dot{v}_L.
\end{aligned}
\tag{14}
$$

Consequently,

$$
\begin{aligned}
\dot{V}_1 = & \varphi_3(t)(\frac{k_{L1}}{\rho} - \frac{k_{L1}^2}{2k_{L2}}) \dot{x}_L^T (N \otimes I_m) \dot{x}_L \\
& + \varphi_3(t)(\frac{k_{L1}}{k_{L2}} \dot{v}_L^T (N \otimes I_m) \dot{v}_L - \frac{k_{L2}}{2} \dot{v}_L^T (N \otimes I_m) \dot{v}_L) \\
& + \frac{k_{L1}}{k_{L2}\rho} \varphi_3(t) \dot{x}_L^T (M \otimes I_m) \dot{v}_L
\end{aligned}
\tag{15}
$$

Applying Lemma 1 and Young's inequality, it is readily concluded that

$$
\begin{aligned}
\lambda_{\min}(N) \dot{x}_L^T \dot{x}_L &\leq \dot{x}_L^T (N \otimes I_r) \dot{x}_L \leq \lambda_{\max}(N) \dot{x}_L^T \dot{x}_L, \\
\dot{x}_L^T (M \otimes I_r) \dot{v}_L &\leq \frac{1}{2} \lambda_{\max}(M)(\dot{x}_L^T \dot{x}_L + \dot{v}_L^T \dot{v}_L).
\end{aligned}
\tag{16}
$$

Substituting (15) into (14) yields

$$
\begin{aligned}
\dot{V}_1 \leq & [(\frac{k_{L1}}{\rho} - \frac{k_{L1}^2}{2k_{L2}}) \lambda_{\max}(N) + \frac{k_{L1}}{2k_{L2}\rho} \lambda_{\max}(M)] \varphi_3(t) \dot{x}_L^T \dot{x}_L \\
& - \frac{k_{L2}}{2} \lambda_{\min}(N) \varphi_3(t) \dot{v}_L^T \dot{v}_L \\
& + \frac{k_{L1}}{k_{L2}} \lambda_{\max}(M)(1 + \frac{1}{2\rho}) \varphi_3(t) \dot{v}_L^T \dot{v}_L
\end{aligned}
\tag{17}
$$

Referring to (15), it can be deduced that

$$
\begin{aligned}
V_1 &\le \frac{k_{L2}}{2}\lambda_{\max}(N)\dot{x}_L^T\dot{x}_L + \frac{1}{2}\lambda_{\max}(M)\dot{v}_L^T\dot{v}_L \\
&+ \frac{k_{L1}}{2k_{L2}}\lambda_{\max}(M)(\dot{x}_L^T\dot{x}_L + \dot{v}_L^T\dot{v}_L) \\
&= (\frac{k_{L1}}{2}\lambda_{\max}(N) + \frac{k_{L1}}{2k_{L2}}\lambda_{\max}(M))\dot{x}_L^T\dot{x}_L \\
&+ (\frac{k_{L1}}{2k_{L2}} + \frac{1}{2})\lambda_{\max}(M)\dot{v}_L^T\dot{v}_L
\end{aligned} \tag{18}
$$

Define $\eta_1(t) = \dot{V}_1 + (c_2 + d_2\varphi_3(t))V_1$, From (10), it indicates that $0 < \frac{1}{\varphi_3(t)} \le \frac{3T_K}{\rho}$. Let $\eta_1(t) \le 0$. It follows that

$$
\begin{aligned}
\eta_1(t) &\le \frac{k_{L1}}{2k_{L2}\rho}[(k_{L2}(2 + 3c_2T_K + d_2\rho) - k_{L1}\rho)\lambda_{\max}(N) \\
&+ (3c_2T_K + d_2\rho)\lambda_{\max}(M)]\dot{x}_L^T\dot{x}_L \\
&+ \frac{1}{2k_{L2}\rho}[-\rho k_{L2}^2\lambda_{\max}(N) + k_{L1}(2\rho+1)\lambda_{\max}(M) \\
&+ (3c_2T_K + d_2\rho)(k_{L1} + k_{L2})\lambda_{\max}(M)]\dot{v}_L^T\dot{v}_L \\
&\le 0
\end{aligned} \tag{19}
$$

We can deduce that the conditions (10) hold. It thus concludes that $\dot{V}_1 \le -c_2 - d_2\varphi_3(t)V_1$. In accordance with Lemma 1, it ensues $V_1 \le \chi_3^{-d_2}(t)\exp(-c_2(t-t_0))V_1(t_0)$. Based on Lemma 1, it obtains $\lim_{t\to T}\chi_3^{-d_2}(t) = 0$, where $T = t_0 + 3T_K$, it further obtains $\lim_{t\to T}\|\dot{x}_L\| = 0$ and $\lim_{t\to T}\|\dot{v}_L\| = 0$. For $t \in [t_0, \infty)$, It can be derived that $V_1 \equiv 0$, thus, it concludes that $\|\dot{x}_L\| = 0$, $\|\dot{v}_L\| = 0$. Namely, the prescribedtime formation tracking is achieved within $T = t_0 + 3T_K$.

Next, it is demonstrated to achieve bipartite containment control within T.

Let $\dot{x} = x_F(t) - (\Lambda^{-1}p \otimes I_m)x_L(t)$, $\dot{v} = v_F(t) - (\Lambda^{-1}p \otimes I_m)v_L(t)$. Define two auxiliary states as

$\ddot{x} = \varphi_3(t)\dot{x}$, $\ddot{v} = \dot{v}$. Upon deriving $\ddot{x}$, it results in

$$
\begin{aligned}
\dot{\ddot{x}} &= \dot{\varphi}_3(t)\dot{x} + \varphi_3(t)\dot{\dot{x}} \\
&= \dot{\varphi}_3(t)\dot{x} + \varphi_3(t)(\dot{x}_F(t) - (\Lambda^{-1}p \otimes I_m)\dot{x}_L(t)) \\
&= \dot{\varphi}_3(t)\dot{x} + \varphi_3(t)(v_F(t) - (\Lambda^{-1}p \otimes I_m)v_L(t)) \\
&= \dot{\varphi}_3(t)\dot{x} + \varphi_3(t)\dot{v}
\end{aligned} \tag{20}
$$

By deriving $\ddot{v}$, it yields

$$
\begin{aligned}
\dot{\ddot{v}} &= \dot{v}_F(t) - (\Lambda^{-1}p \otimes I_m)\dot{v}_L(t) \\
&= -k_{F1}\varphi_3^2(t)((\Lambda \otimes I_m)x_F - (p \otimes I_m)x_L) \\
&\quad - k_{F2}\varphi_3(t)((\Lambda \otimes I_m)v_F - (p \otimes I_m)v_L) \\
&= -k_{F1}\varphi_3^2(t)((\Lambda \otimes I_m)\dot{x}) - k_{F2}\varphi_3(t)((\Lambda \otimes I_m)\dot{v}) \\
&= -k_{F1}\varphi_3(t)(\Lambda \otimes I_m)\ddot{x} - k_{F2}\varphi_3(t)((\Lambda \otimes I_m)\ddot{v}) \\
&= -\varphi_3(t)(\Lambda \otimes I_m)(k_{F1}\ddot{x} + k_{F2}\ddot{v})
\end{aligned}
$$

Define $X = [\ddot{x}^T, \ddot{v}^T]^T$, it follows that $\dot{X} = \Xi X$, where

$$\Xi = \begin{bmatrix} \dot{\varphi}_3(t)I_n & \varphi_3(t)I_n \\ -k_{F1}\varphi_3(t)\Lambda & -k_{F2}\varphi_3(t)\Lambda \end{bmatrix} \otimes I_r \tag{21}$$

The Lyapunov function candidate is defined as $V = \dfrac{1}{2}X^T(\Psi \otimes I_r)X$, where $\Psi = \begin{bmatrix} k_{F1}N & \dfrac{k_{F1}}{k_{F2}}M \\ \dfrac{k_{F1}}{k_{F2}}M & M \end{bmatrix}$,

N, M are defined in Lemma 2. From Lemma 2, it obtains that M is positive define, then according to the fourth inequality of (10), it follows that $V \geq 0$.

Taking the derivative of V with respect to time, it follows that

$$\begin{aligned}
\dot{V} &= \frac{k_{F1}}{\rho}\varphi_3(t)\dot{x}^T(N \otimes I_r)\dot{x} - \frac{k_{F1}^2}{k_{F2}}\varphi_3(t)\dot{x}^T(\Lambda M \otimes I_r)\dot{x} \\
&\quad + \frac{k_{F1}}{k_{F2}}\varphi_3(t)\dot{v}^T(M \otimes I_r)\dot{v} - k_{F2}\varphi_3(t)\dot{v}^T(\Lambda M \otimes I_r)\dot{v} \\
&\quad + \dot{x}^T(k_{F1}\varphi_3(t)(N \otimes I_r) + \frac{k_{F1}}{k_{F2}\rho}\varphi_3(t)(M \otimes I_r))\dot{v} - k_{F1}\varphi_3(t)\dot{x}^T(N \otimes I_r)\dot{v}
\end{aligned} \tag{22}$$

Utilizing Lemma 2, the following equality is established.

$$\begin{aligned}
\frac{k_{F1}^2}{k_{F2}}\varphi_3(t)\dot{x}^T(\Lambda M \otimes I_r)\dot{x} &= \frac{k_{F1}^2}{2k_{F2}}\varphi_3(t)\dot{x}^T(N \otimes I_r)\dot{x} \\
k_{F2}\varphi_3(t)\dot{v}^T(\Lambda M \otimes I_r)\dot{v} &= \frac{k_{F2}}{2}\varphi_3(t)\dot{v}^T(N \otimes I_r)\dot{v}
\end{aligned} \tag{23}$$

It thus follows

$$\begin{aligned}
\dot{V} &= \varphi_3(t)(\frac{k_{F1}}{\rho} - \frac{k_{F1}^2}{2k_{F2}})\dot{x}^T(N \otimes I_r)\dot{x} \\
&\quad + \varphi_3(t)(\frac{k_{F1}}{k_{F2}}\dot{v}^T(M \otimes I_r)\dot{v} - \frac{k_{F2}}{2}\dot{v}^T(N \otimes I_r)\dot{v}) + \frac{k_{F1}}{k_{F2}\rho}\varphi_3(t)\dot{x}^T(M \otimes I_r)\dot{v}
\end{aligned} \tag{24}$$

Drawing upon Lemma 2 and Young's inequality, it can be readily concluded that

$$\begin{aligned}
\lambda_{\min}(N)\dot{x}^T\dot{x} &\leq \dot{x}^T(N \otimes I_r)\dot{x} \leq \lambda_{\max}(N)\dot{x}^T\dot{x} \\
\dot{x}^T(M \otimes I_r)\dot{v} &\leq \frac{1}{2}\lambda_{\max}(M)(\dot{x}^T\dot{x} + \dot{v}^T\dot{v})
\end{aligned} \tag{25}$$

Substituting (24) into (23) yields

$$\begin{aligned}
\dot{V} &\leq [(\frac{K_{F1}}{\rho} - \frac{K_{F1}^2}{2K_{F2}})\lambda_{\max}(N) + \frac{K_{F1}}{2K_{F2}\rho}\lambda_{\max}(M)]\varphi_3(t)\dot{x}^T\dot{x} \\
&\quad - \frac{K_{F2}}{2}\lambda_{\min}(N)\varphi_3(t)\dot{v}^T\dot{v} + \frac{K_{F1}}{K_{F2}}\lambda_{\max}(M)(1 + \frac{1}{2\rho})\varphi_3(t)\dot{v}^T\dot{v}
\end{aligned} \tag{26}$$

Referring to (24), it can be deduced that

$$V \leq \frac{K_{F2}}{2}\lambda_{\max}(N)\tilde{x}^T\tilde{x} + \frac{1}{2}\lambda_{\max}(M)\tilde{v}^T\tilde{v} + \frac{K_{F1}}{2K_{F2}}\lambda_{\max}(M)(\tilde{x}^T\tilde{x} + \tilde{v}^T\tilde{v})$$

$$= (\frac{K_{F2}}{2}\lambda_{\max}(N) + \frac{K_{F1}}{2K_{F2}}\lambda_{\max}(M))\tilde{x}^T\tilde{x} + (\frac{1}{2} + \frac{K_{F1}}{2K_{F2}})\lambda_{\max}(M)\tilde{v}^T\tilde{v} \quad (27)$$

Define $\eta(t) = \dot{V} + (c + d\varphi(t))V$. Let $\eta(t) \leq 0$. It follows that

$$\eta(t) \leq \frac{K_{F1}}{2K_{F2}\rho}[(K_{F2}(2+3cT+d\rho) - K_{F1}\rho)\lambda_{\max}(N) + (3cT+d\rho+1)\lambda_{\max}(M)]\tilde{x}^T\tilde{x}$$

$$+ \frac{1}{2K_{F2}\rho}[-\rho K_{F2}^2\lambda_{\min}(N) + K_{F1}(2\rho+1)\lambda_{\max}(M) + (3cT+d\rho)(K_{F1}+K_{F2})\lambda_{\max}(M)]\tilde{v}^T\tilde{v} \leq 0$$

It can be inferred that the conditions (10) hold. Consequently, it concludes that $\dot{V} \leq -cV - d\varphi_3(t)V$, According to Lemma 1, it follows $V \leq \chi_3^{-d}(t)\exp(-c(t-t_0))V(t_0)$. Based on Lemma 1, it obtains $\lim_{t \to T}\chi_3^{-d}(t) = 0$, where $T = t_0 + 3T_K$, it further obtains $\lim_{t \to T}\|\tilde{x}\| = 0$ and $\lim_{t \to T}\|\tilde{v}\| = 0$. For $t \in [t_0, \infty)$, it can be obtained that $V \equiv 0$, It thus concludes that $\|\tilde{x}\| = 0$, $\|\tilde{v}\| = 0$. Namely, the prescribedtime bipartite containment is achieved within $T = t_0 + 3T_K$.

IV.SIMULATION

To evaluate of the effectiveness of the proposed algorithms, we perform simulations using the multi-agent networks with nine agents. The systems comprise one tracking leader, four formation leaders and four followerswith the signed communication digraph G depicted in fig1.These relationships correspond to the adjacency matrix of points:
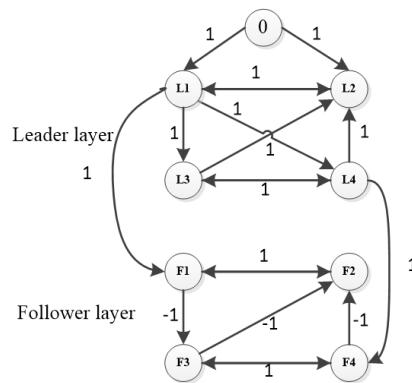

Fig.1. Communication topology

$$B = \begin{pmatrix} 0 & 1 & 0 & 0 \\ 1 & 0 & 1 & 1 \\ 1 & 0 & 0 & 1 \\ 1 & 0 & 1 & 0 \end{pmatrix}, \quad A = \begin{pmatrix} 0 & 1 & 0 & 0 \\ 1 & 0 & -1 & -1 \\ -1 & 0 & 0 & 1 \\ 0 & 0 & 1 & 0 \end{pmatrix}, \quad p = diag(1,0,0,-1), G = diag(1,1,0,0).$$ There is a restraining

relationship between the agent 1 and agent 4 in the leader layer and the agent 1 and agent 4 in the follower layer, which is represented as the **Error! Reference source not found.**. Follower agent layer can be divided into two groups: $v_1^2 = \{1,2\}$ $v_2^2 = \{3,4\}$ .We have:

$\eta^L = \{(1,2),(2,1),(3,1),(2,4),(3,4),(4,3),(2,3),(4,1)\}$, $\eta^F = \{(1,2),(2,1),(3,1),(2,4),(3,4),(4,3),(2,3)\}$, and it follows that $\eta^L \in \eta^F$, while η^L is not equal to η^F .Thus Assumption 2 holds.

Let $\rho = 6$, $t_0 = 0s$, $T_K = 0.75$, $K_{L1} = 60$, $K_{L2} = 30$, $K_{F1} = 0.01$, $K_{F2} = 60$, $c_1 = 0.1$, $d_1 = 50$, $\beta = 0.5$. The virtual leader serves the purpose of furnishing trajectory guidance for all the followers. The trajectory of the virtual leader is delineated as

$$\begin{cases} x_0 = [2 + 4\cos(0.5t), -1 + 4\sin(0.5t)]^T \\ v_0 = [-2\sin(0.5t), 2\cos(0.5t)]^T \\ u_0 = [-\cos(0.5t), -\sin(0.5t)]^T \end{cases}$$
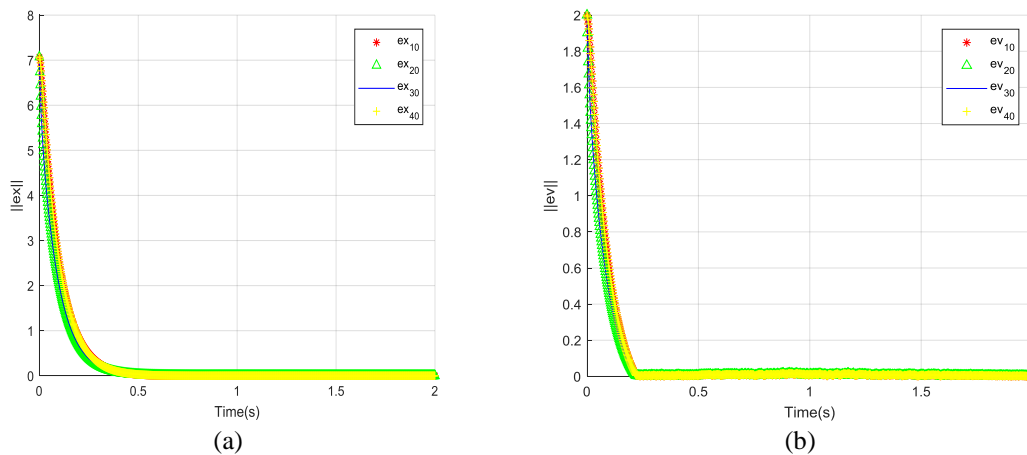

(a)   (b)

Fig. 2. Pictures (a) and (b) show the observer errors ς_x and ς_v converge to zero within the prescribedtime $t_0 + T_K$ and $t_0 + 2T_K$, respectively.

The initial values of x_{fi} , x_{li} , v_{fi} , v_{li} , ς_{xi} , ς_{vi} are selected randomly. the simulation results are shown in Figs. 2–6. Fig. 2 shows that the observer errors ς_x and ς_v converge to zero within the prescribedtime $t_0 + T_K$ and $t_0 + 2T_K$, respectively. Fig. 3-Fig. 6 are the drawing of agents in different time, within a specified time, the convex hull formed by leaders is indicated by solid lines. Follower 1 and 2 in the square formed by leaders, follower 3 and 4 into the square, which is formed by the symbolic opposite state of the leaders is marked by dotted lines. From Fig. 6, it can be observed that the positions of the leaders maintain the desired regular square formation, and the positions of the followers remain within the convex hull formed by the leader positions in both the simulation and the experiment. Therefore, the specified time control protocol control is achieved.
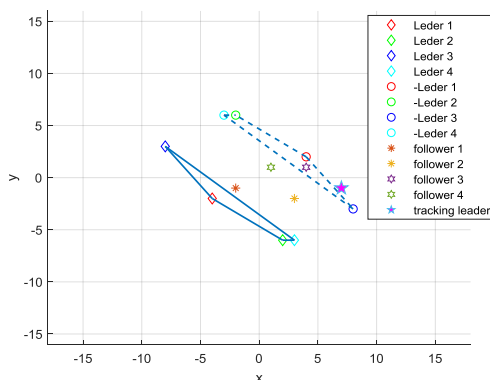

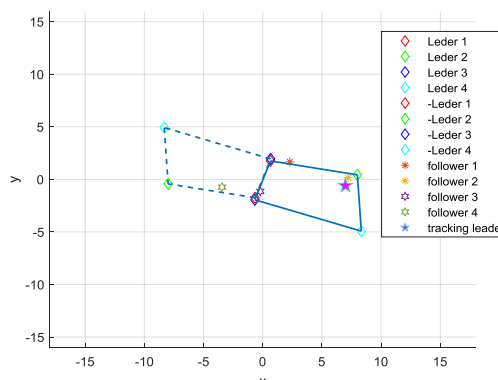Fig.3. The trajectory of each agent at $t = 0s$ Fig.4. The trajectory of each agent at $t = 0.198s$
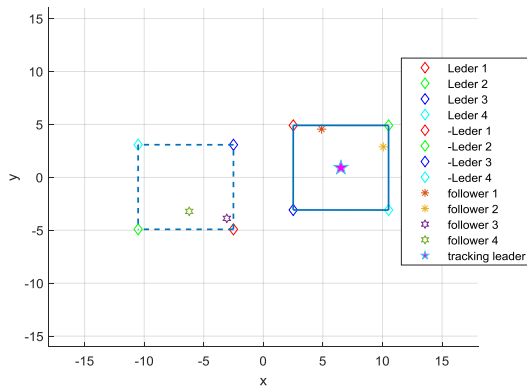
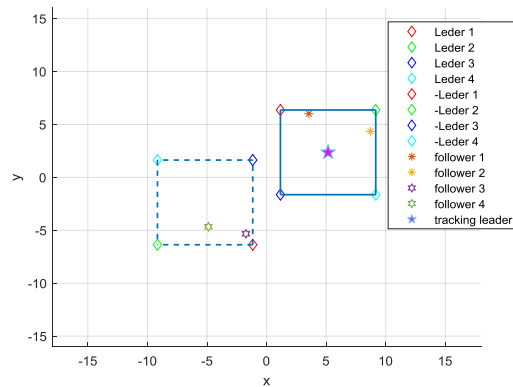Fig.5. The trajectory of each agent at $t = 0.998s$

Fig.6. The trajectory of each agent at $t = 2s$

V. CONCLUSION

This paper has investigated the bipartite formation-containment tracking control of a class of two-layered MASs under signed graphsbased on the observer. A new state observer has been developed to estimate the unmeasurable state of the tracking leader within a prescribed time, which can be predetermined by freely adjusting a time-independent parameter. Subsequently,a novel prescribed time distributed control protocol has been devised to effectively address the bipartite formation-containment problembased on prescribedtime observers. The simulation and experimental results were provided to illustrate the effectiveness of the obtained results.

REFERENCES

[1]   Li Y, Tan C. A survey of the consensus for multi-agent systems. Systems Science & Control Engineering, 2019, 7(1): 468-482.
[2]   Mousavi A, Markazi A H D. A new control method for leader-follower consensus problem of uncertain constrained nonlinear multi-agent systems. Journal of the Franklin Institute, 2024: 106889.
[3]   Dong X, Zhou Y, Ren Z, et al. Time-varying formation tracking for second-order multi-agent systems subjected to switching topologies with application to quadrotor formation flying. IEEE Transactions on Industrial Electronics, 2016, 64(6): 5014-5024.
[4]   Enwerem C, Baras J S. Formation Tracking for a Class of Uncertain Multi-Agent Systems: A Distributed Kalman Filtering Approach. IEEE Control Systems Letters, 2024,8: 217-222.
[5]   Wang Y, Han L, Li X, et al. Time-varying formation tracking for multi-agent systems with maneuvering leader under DDoS attacks and actuator faults. ISA transactions, 2024, 144: 38-50.
[6]   Zou W, Huang Y, Ahn C. K, et al. Containment control of linear multiagent systems with stochastic disturbances via event-triggered strategies. IEEE Systems Journal, 2020, 14(4), 4810-4819.
[7]   Liu, Y, Zhang J, and Jia Y. Adaptive containment control of heterogeneous high-order fully actuated multi-agent systems. International Journal of Robust and Nonlinear Control, 2024, 34(7): 4802-4819.
[8]   Chen L, Li C, Guo Y, et al. Formation–containment control of multi-agent systems with communication delays. ISA transactions, 2022, 128: 32-43.
[9]   Hua Y, Dong X, Han L, et al. Formation-containment tracking for general linear multi-agent systems with a tracking-leader of unknown control input. Systems & control letters, 2018, 122: 67-76.
[10]   González-Sierra J, Ramirez-Neria M, Santiaguillo-Salinas J, et al. Saturated formation containment control for a heterogeneous multi-agent system with unknown perturbations. Automatica, 2024, 159: 111343.
[11]   Han L, Dong X, Li Q, et al. Formation-containment control for second-order multi-agent systems with time-varying delays. Neurocomputing, 2016, 218: 439-447.
[12]   Liao R, Han L, Dong X, et al. Finite-time formation-containment tracking for second-order multi-agent systems with a virtual leader of fully unknown input. Neurocomputing, 2020, 415: 234-246.
[13]   Bi C, Xu X, Liu L, et al. Formation-containment tracking for heterogeneous linear multi-agent systems under unbounded distributed transmission delays. IEEE Transactions on Control of Network Systems, 2022, 10(2), 822-833.
[14]   Yuan C, Yan H, Wang Y, et al. Formation-containment control of heterogeneous linear multi-agent systems with adaptive event-triggered strategies. International Journal of Systems Science, 2022, 53(9): 1942-1957.
[15]   Zhang M, Sun Y, Liu H, et al. Event-triggered formation-containment control for multi-agent systems based on sliding mode control approaches. Neurocomputing, 2023, 562: 126905.
[16]   Yu D, Ge S S, Li D, et al. Finite-horizon robust formation-containment control of multi-agent networks with unknown dynamics. Neurocomputing, 2021, 458: 403-415.
[17]   Zhang H, Chen J. Bipartite consensus of multi‐agent systems over signed graphs: state feedback and output feedback control approaches. International Journal of Robust and Nonlinear Control, 2017, 27(1): 3-14.
[18]   Wen G, Jiang D, Peng Z, et al. Fully Distributed Bipartite Formation Control for Stochastic Heterogeneous Multi-Agent Systems Under Signed Markovian Switching Topology. IEEE Transactions on Control of Network Systems, 2024:1-10.
[19]   Altafini C. Consensus problems on networks with antagonistic interactions. IEEE transactions on automatic control, 2012, 58(4): 935-946.
[20]   Wen G, Yu W, Zhao Y, et al. Node-to-node consensus of networked agents with general linear node dynamics//2013 IEEE International Conference on Cyber Technology in Automation, Control and Intelligent Systems. IEEE, 2013: 24-29.
[21]   Wand Y, Hu A. Consensus of two-layer multi-agent systems subjected to cyber-attack. Journal of Computer Applications, 2021, 41(5):

1399-1405.

[22]   Wen G, Wang P, Huang T, et al. Distributed consensus of layered multi-agent systems subject to attacks on edges. IEEE Transactions on Circuits and Systems I: Regular Papers, 2020, 67(9): 3152-3162.

[23]   Hua Y, Dong X, Han L, et al. Finite-time time-varying formation tracking for high-order multiagent systems with mismatched disturbances. IEEE Transactions on Systems, Man, and Cybernetics: Systems, 2018, 50(10): 3795-3803.

[24]   Zhang X, Wu J, Zhan X, et al. Observer-based adaptive time-varying formation-containment tracking for multiagent system with bounded unknown input. IEEE Transactions on Systems, Man, and Cybernetics: Systems, 2022, 53(3): 1479-1491.

[25]   Wen G, Yu X, Fu J, et al. Fast distributed average tracking in multiagent networks: The case with general linear agent dynamics. IEEE Transactions on Control of Network Systems, 2020, 8(2): 997-1009.

[26]   Xiong T, Gu Z. Observer-based adaptive fixed-time formation control for multi-agent systems with unknown uncertainties. Neurocomputing, 2021, 423: 506-517.

[27]   Ding T F, Ge M F, Xiong C, Liu Z W, et al. Prescribed-time formation tracking of second-order multi-agent networks with directed graphs. Automatica, 2023, 152: 110997.